BBA - Molecular Basis of Disease 1868 (2022) 166530

Contents lists available at ScienceDirect

BBA - Molecular Basis of Disease

journal homepage: www.elsevier.com/locate/bbadis

Itaconate controls its own synthesis via feedback-inhibition of reverse TCA cycle activity at IDH2

Alexander Heinz [a], Yannic Nonnenmacher [a], Antonia Henne [a], Michelle-Amirah Khalil [a], Ketlin Bejkollari [a], Catherine Dostert [b], Shirin Hosseini [c], Oliver Goldmann [d], Wei He [a], Roberta Palorini [e], Charlène Verschueren [b], Martin Korte [c,f], Ferdinando Chiaradonna [e], Eva Medina [d], Dirk Brenner [b,g,h], Karsten Hiller [a,*]

[a] Department for Bioinformatics and Biochemistry, BRICS, Technische Universität Braunschweig, Rebenring 56, 38106 Braunschweig, Germany
[b] Experimental and Molecular Immunology, Department of Infection and Immunity, Luxembourg Institute of Health, Esch-sur-Alzette, Luxembourg
[c] Department of Cellular Neurobiology, Zoological Institute, Technische Universität Braunschweig, Germany
[d] Infection Immunology Research Group, Helmholtz Centre for Infection Research, Braunschweig, Germany
[e] Department of Biotechnology and Biosciences, University of Milano-Bicocca, Piazza della Scienza, Milan, Italy
[f] Neuroinflammation and Neurodegeneration Research Group, Helmholtz Centre for Infection Research, Braunschweig, Germany
[g] Immunology and Genetics, Luxembourg Centre for System Biomedicine (LCSB), University of Luxembourg, Belval, Luxembourg
[h] Odense Research Center for Anaphylaxis, Department of Dermatology and Allergy Center, Odense University Hospital, University of Southern Denmark, Odense, Denmark

ARTICLE INFO

Keywords:
Proinflammatory macrophage
TCA cycle
Reductive carboxylation
Mitochondrial metabolism
Redox balance
2-hydroxyglutarate

ABSTRACT

Macrophages undergo extensive metabolic reprogramming during classical pro-inflammatory polarization (M1-like). The accumulation of itaconate has been recognized as both a consequence and mediator of the inflammatory response. In this study we first examined the specific functions of itaconate inside fractionated mitochondria. We show that M1 macrophages produce itaconate de novo via aconitase decarboxylase 1 (ACOD1) inside mitochondria. The carbon for this reaction is not only supplied by oxidative TCA cycling, but also through the reductive carboxylation of α-ketoglutarate by isocitrate dehydrogenase (IDH). While macrophages are capable of sustaining a certain degree of itaconate production during hypoxia by augmenting the activity of IDH-dependent reductive carboxylation, we demonstrate that sufficient itaconate synthesis requires a balance of reductive and oxidative TCA cycle metabolism in mouse macrophages. In comparison, human macrophages increase itaconate accumulation under hypoxic conditions by augmenting reductive carboxylation activity. We further demonstrated that itaconate attenuates reductive carboxylation at IDH2, restricting its own production and the accumulation of the immunomodulatory metabolites citrate and 2-hydroxyglutarate. In line with this, reductive carboxylation is enhanced in ACOD1-depleted macrophages. Mechanistically, the inhibition of IDH2 by itaconate is linked to the alteration of the mitochondrial $NADP^+$/NADPH ratio and competitive succinate dehydrogenase inhibition. Taken together, our findings extend the current model of TCA cycle reprogramming during pro-inflammatory macrophage activation and identified novel regulatory properties of itaconate.

1. Introduction

As part of the innate immune system, macrophages play a crucial role in mounting the immune response. In response to infection-associated stimuli such as bacterial lipopolysaccharide (LPS), macrophages are rapidly activated into the proinflammatory phenotype, accompanied by a tightly controlled transcriptional and metabolic reprogramming. Activated macrophages undergo a Warburg-like metabolic switch from oxidative phosphorylation to aerobic glycolysis, in order to meet the prompt and increased energy demand to synthesize inflammatory cytokines [1]. Mechanistically, macrophages attenuate the activity of multiple TCA cycle enzymes as they require less reducing equivalents for respiration, which has been described previously as a "broken TCA cycle" [2]. However, it has become clear that the TCA cycle is not merely

* Corresponding author.
E-mail address: karsten.hiller@tu-braunschweig.de (K. Hiller).

https://doi.org/10.1016/j.bbadis.2022.166530
Received 31 May 2022; Received in revised form 11 August 2022; Accepted 17 August 2022
Available online 28 August 2022

attenuated, but reprogrammed to increase the production of multiple immunomodulatory metabolites. Among these, the synthesis of TCA-cycle derived itaconate via the inducible enzyme aconitase decarboxylase 1 (ACOD1) has attracted widespread attention as a hallmark of LPS-stimulated macrophages "M(LPS)" [3]. Itaconate is readily transported into the lysosomes and limits the growth of pathogens by inhibition of the glyoxylate shunt enzyme isocitrate lyase [4]. A plethora of immunoregulatory functions have been attributed to itaconate, most notably the inhibition of succinate dehydrogenase (SDH) leading to the accumulation of succinate and stabilization of transcription factor hypoxia-inducible factor-1α (HIF-1α) [1,5]. The anti-inflammatory effects of itaconate have been extensively studied using either ACOD1-deficient macrophages or esterified itaconate derivatives dimethyl itaconate and 4-octyl-itaconate [1]. While these cell-permeable derivatives attenuate the inflammatory response of macrophages through alkylation of multiple target proteins including KEAP1, ATF3 and GAPDH [6–8], recent studies questioned whether these findings can in fact be extrapolated to unmodified itaconate [9,10]. Mesaconate, a putative intermediate during the degradation of itaconate, has also recently been identified as an immunomodulatory metabolite in activated macrophages [10].

Isocitrate dehydrogenase 1 (IDH1, cytosolic) and 2 (IDH2, mitochondrial) are $NADP^+$-dependent TCA cycle enzymes, which catalyze the interconversion between isocitrate and α-ketoglutarate (α-KG). Expression levels of *Idh1* and *Idh2* are potently reduced during prolonged LPS stimulation in macrophages, which has been termed a TCA cycle break allowing the redirection of TCA cycle carbon towards itaconate synthesis [11,12]. However, recent studies questioned this view, as M(LPS) macrophages rapidly produce high amounts of nitric oxide (NO), an inhibitor of the TCA cycle enzyme aconitase (ACO) and pyruvate dehydrogenase (PDH) [13]. In fact, incorporation of glucose-derived carbon into itaconate is very low in WT macrophages, but strongly elevated in *Nos2*-deficient macrophages [13]. As the TCA cycle break at ACO favors citrate accumulation over itaconate synthesis, the question arises how M(LPS) macrophages maintain the synthesis of itaconate. $NADP^+$-dependent IDH isoforms have been shown to catalyze the reductive carboxylation of α-KG to citrate, a process which is elevated under impaired mitochondrial respiration, hypoxia or in the context of cancer metabolism to synthesize citrate with glutamine-derived carbon [14,15]. Intriguingly, an increase in reductive carboxylation activity in M(LPS) macrophages was not observed in previous publications [11,16], which could be attributed to the decreased expression of NADPH-dependent IDH and NO-dependent inhibition of ACO. However, reductive metabolism should be energetically favorable for M(LPS) macrophages, which maintain the oxidation of glutamine-derived carbon in the TCA cycle [16,17] despite attenuated oxidative phosphorylation [18] and display an overly reduced redox balance [19], driving the need for alternative ways of NAD(*P*)H oxidation. Tissue hypoxia, an important environmental factor for inflammatory macrophages [20], might further increase the need for the re-oxidation of reduced co-factors. Despite recent advances, a comprehensive understanding of the temporal-spatial changes during metabolic reprogramming in M(LPS) macrophages has not emerged yet. To remedy this, we were interested to further decipher mitochondrial metabolism in M(LPS) macrophages with a particular focus on redox and hypoxia biology, the temporality of metabolic reprogramming and interspecies differences. To specifically profile mitochondrial immunometabolism, we employed a recently developed method for the selective permeabilization of the cytosolic membrane to study mitochondrial metabolism in situ [21]. This assay enables the profiling of mitochondrial metabolism independently of transcriptional regulation and allows for the rapid uptake and functional profiling of extracellular compounds like itaconate.

2. Results

2.1. Itaconate and mesaconate are synthesized in macrophage mitochondria

Immunological activation of M(LPS) macrophages is accompanied by a reprogramming of cellular and mitochondrial metabolism to support macrophage function [1]. To analyze how this activation specifically affects mitochondrial metabolism in situ, we performed a selective permeabilization of the cytosolic membrane with digitonin (Fig. 1A and B). We first were interested to test if fractionated mitochondria can synthesize itaconate and mesaconate from the mitochondrial energy metabolites pyruvate and glutamine. Following permeabilization of M(LPS) RAW 264.7 macrophages, we incubated fractionated mitochondria with 1 mM of each pyruvate and glutamine as the sole carbon sources. Mitochondrial itaconate levels increased substantially over the course of 45 min of incubation (Fig. 1C). To validate if the synthesis is indeed de novo, we employed stable-isotope labeled [U-^{13}C]-glutamine as a tracer (Fig. 1D). Assuming an active and complete itaconate synthesis pathway within mitochondria, ^{13}C carbon isotopes from [U—^{13}C]-glutamine will be incorporated into *cis*-aconitate and, after decarboxylation by ACOD1, into itaconate. Time-resolved analysis of M4 citrate and itaconate mass isotopomers revealed the mitochondrial de novo synthesis of both metabolites (Fig. 1E). Isotopic enrichment in citrate was faster as in itaconate, confirming that itaconate is produced downstream of citrate via the ACO- and ACOD1-catalyzed reactions. We confirmed the presence of ACOD1 in mitochondria by Western blot and further demonstrated that digitonin treatment induces complete separation of cytosolic (GAPDH) and mitochondrial (VDAC1) proteins (Fig. 1F). Recently, an isomer of itaconate, the carboxylic acid mesaconate, was reported to be produced in M(LPS) macrophages downstream of itaconate [10]. Mesaconate exerts similar immunomodulatory functions like itaconate and might be an intermediate during the degradation of itaconate. In addition to itaconate synthesis, we observed mitochondrial mesaconate production and the incorporation of ^{13}C carbon isotopes from [U—^{13}C]-glutamine followed a similar pattern than that of citrate and itaconate (Fig. 1E). Based on the slower increase of M4 mesaconate isotopologues, we conclude that it is produced downstream of itaconate.

Apart from its anti-bacterial functions [3], itaconate has been shown to act as a competitive inhibitor of SDH (succinate dehydrogenase) [5]. Since SDH is a key enzyme in mitochondrial metabolism, we were interested to profile the impact of itaconate directly in fractionated mitochondria of human monocyte-derived macrophages (hMDMs) and RAW 264.7 macrophages. We profiled the metabolic response of macrophage mitochondria to the treatment with itaconate and compared these results to two other SDH inhibitors, malonate and 3-nitropropionate (3-NPA) (Fig. 1G). While each compound increased mitochondrial succinate levels, indicative of their inhibitory effect on SDH, itaconate induced a comparatively weak effect on the mitochondrial TCA cycle metabolome, albeit at higher concentrations than malonate or 3-NPA. Intriguingly, treatment with itaconate affected aspartate levels differently in mouse and human macrophages, as aspartate accumulated in RAW 264.7 mitochondria, while it was depleted in hMDM mitochondria. Similar to the treatment with itaconate, mitochondria of M(LPS) RAW 264.7 macrophages accumulated higher amounts of succinate, indicating that endogenous mitochondrial itaconate production is sufficient to inhibit SDH (Fig. 1H). To profile the activity of oxidative TCA cycle metabolism, we applied a [U—^{13}C]-glutamine tracer and quantified the fraction of M3 (second round) and M5 (first round) α-KG isotopologues (Fig. 1D). We compared the oxidative TCA cycle activity between whole cell macrophages and macrophage mitochondria and observed that the stimulation with LPS reduced the ratio M3 to M5 α-KG to a much greater extent in whole cell macrophages (Fig. 1I). We speculated that fractionated mitochondria from LPS-stimulated RAW 264.7 macrophages are capable of

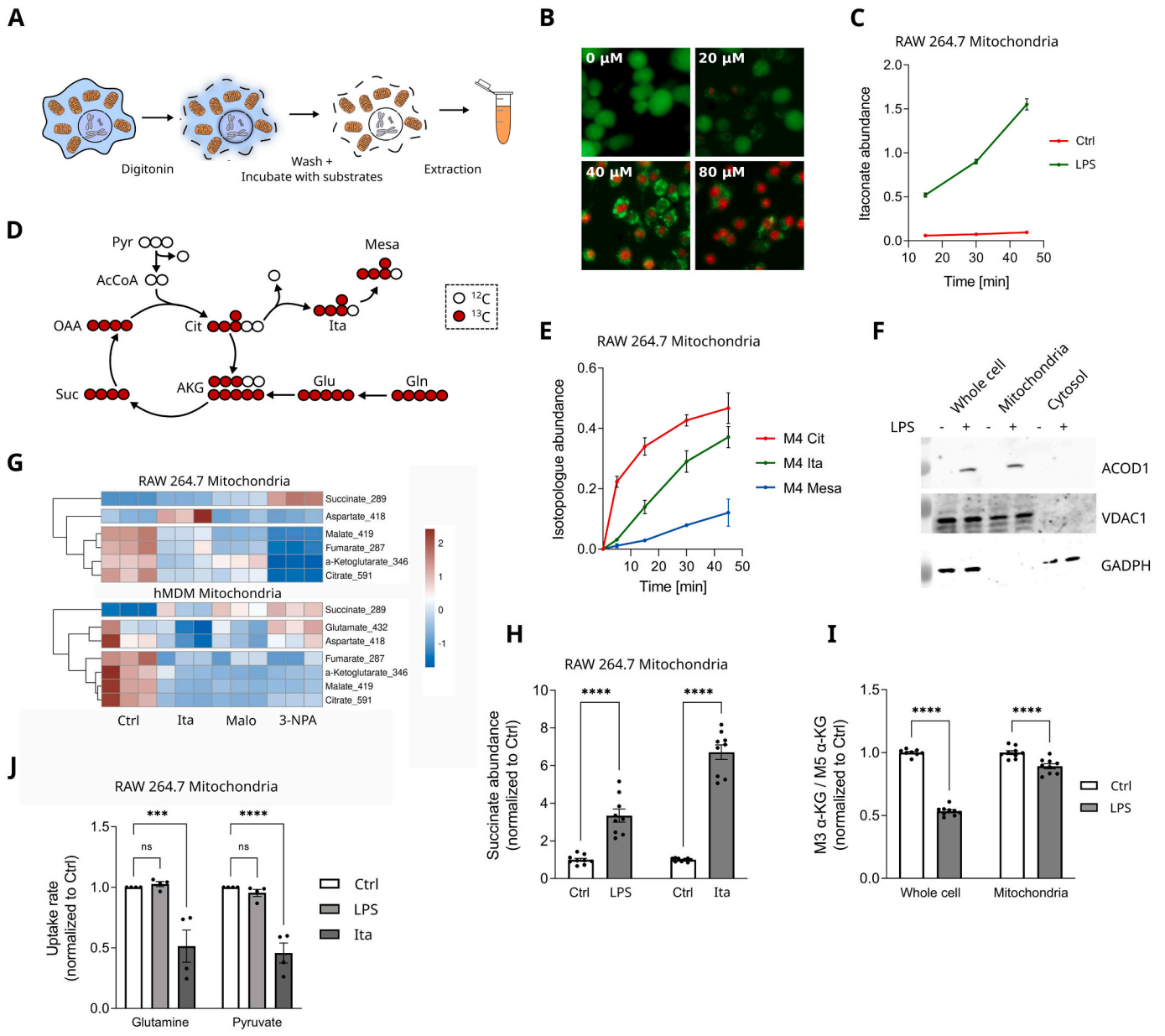

Fig. 1. Compartment-specific analysis of itaconate metabolism. A. Selective permeabilization of cytosolic membrane with digitonin. B. Live/dead cell staining of RAW 264.7 macrophages treated with indicated digitonin concentration. C. Time-resolved itaconate accumulation in mitochondria of RAW 264.7 macrophages pre-treated with 10 ng/ml lipopolysaccharide (LPS) for 6 h. D. TCA cycle atom transitions from [U—^{13}C]-glutamine tracer. E. Relative time-resolved increase of M4 isotoplogues in mitochondria of RAW 264.7 macrophages labeled with [U-^{13}C]-glutamine and pre-treated with 10 ng/ml LPS for 6 h. F. Western blot of whole cell, cytosolic and mitochondrial contents of RAW 264.7 macrophages treated with LPS for 6 h. Volate-dependent anion-selective channel 1 (VDAC1) localizes to the mitochondria and glyceraldehyde 3-phosphate dehydrogenase (GAPDH) is a cytosolic protein. G. Targeted metabolome of RAW 264.7 macrophage or human monocyte-derived macrophage (hMDM) mitochondria following treatment with 10 mM itaconate, 0.5 mM malonate or 0.1 mM 3-nitropropionate (3-NPA) for 30 min. H. Relative succinate levels in mitochondria of RAW 264.7 macrophages treated with 10 mM itaconate for 30 min, or pre-treated with LPS for 6 h. I. Ratio of M3 to M5 α-ketoglutarate (α-KG) in mitochondria of RAW 264.7 macrophages labeled with [U-^{13}C]-glutamine and pre-treated with 10 ng/ml LPS for 6 h. J. Relative uptake of glutamine and pyruvate by mitochondria of RAW 264.7 macrophages treated with 10 mM itaconate for 30 min, or pre-treated with 10 ng/ml LPS for 6 h. All data are presented as mean+/-SEM calculated from (E,H,I) n = 3 replicates from 3 independent experiments or (C,G) n = 3 replicates from a representative experiment of all 3 independent experiments or (F) n = 1 replicate from a representative experiment from all 3 independent experiments or (J) n = 6 replicates from 4 independent experiments. * $P < 0.05$, ** $P < 0.01$, *** $P < 0.001$, **** $P < 0.0001$ calculated by two-way ANOVA with Šidák post-test (H,I,J).

maintaining a high degree of oxidative TCA cycling, which was consistent with the unmodified uptake of mitochondrial energy substrates under these conditions (Fig. 1J). Whole cell macrophages are subjected to cytosol-derived factors like NO [13], which are capable of impairing oxidative TCA cycling, indicating that a combination of itaconate and other factors are necessary to limit oxidative TCA cycling. We therefore conclude that M(LPS) macrophage mitochondria produce itaconate de novo, which triggers the accumulation of succinate, without inducing a quantitative break in the oxidative TCA cycle.

2.2. *Itaconate is synthesized via bidirectional TCA cycle metabolism*

The mitochondrial redox potential is determined by the ratio of NADH and NAD$^+$ and under normal conditions the electron transport chain (ETC) maintains a stable equilibrium by oxidizing reduced NADH that accumulates during oxidative TCA metabolism. However, in

situations of reduced ETC activity, certain TCA cycle enzymes can compensate for this and increase their reductive activity. In fact, hypoxic conditions, or impairments of mitochondrial respiration, promote reductive carboxylation by IDH to produce isocitrate and citrate from glutamine-derived α-KG [15,22]. The reductive carboxylation of α-KG to isocitrate has been shown to be primarily catalyzed by the $NADP^+$-dependent isoforms IDH1 (cytosolic) and IDH2 (mitochondrial) [15]. As mitochondrial reductive carboxylation of α-KG contributes to the synthesis of *cis*-aconitate and thus intersects with the pathway for itaconate production, we hypothesized that reductive IDH activity could be involved in the de novo production of itaconate in mitochondria of M(LPS) macrophages. While the application of [U-^{13}C]-glutamine allows to distinguish oxidatively produced (M4) and reductive carboxylation-derived (M5) citrate, it fails to resolve the fractional contribution of itaconate production, as both directions of the TCA cycle give rise to M4 itaconate (Fig. 2A). To overcome this limitation, we employed [1-^{13}C]-glutamine, which selectively labels reductive carboxylation-derived itaconate. We first treated M(LPS) RAW 264.7 macrophages with [1-^{13}C]-glutamine and determined the ratio of M1 citrate or M1 itaconate to M1 α-KG to quantify the flux of reductive carboxylation-derived *cis*-aconitate to citrate by ACO, or to itaconate by ACOD1 (Fig. 2B). Interestingly, we observed a much higher ratio of M1 itaconate to M1 α-KG, demonstrating the preferred decarboxylation of *cis*-aconitate to itaconate. Expectedly, we observed that hypoxic LPS-stimulated RAW 264.7 macrophages further augmented the reductive production of itaconate and citrate. The comparatively lower ratio of M1 citrate to M1 α-KG indicates that the reductive flux through cytosolic IDH1 to itaconate, which passes through citrate, is not the primary pathway for reductive itaconate synthesis. To validate that mitochondrial IDH2 is the predominant isoform involved in reductive itaconate production, we treated IDH1 or IDH2 silenced RAW 264.7 macrophages with LPS and [1-^{13}C]-glutamine and measured the flux from α-KG to itaconate (Fig. 2C). As speculated, the knock-down of IDH2 induced a stronger decrease in reductive itaconate production than the knock-down of IDH1.

We next estimated the fraction of reductive and oxidative (first round of TCA cycling) glutamine-dependent itaconate synthesis in M(LPS) macrophages by utilizing a combination of [1-^{13}C]-glutamine and [U-^{13}C]-glutamine (Fig. 2D). Under normoxic conditions, reductive carboxylation accounted for 35–40 % of glutamine-derived itaconate in M(LPS) RAW 264.7 macrophages. Although tumor cells are known for higher reductive carboxylation activity [15], we observed similar contributions in mouse bone marrow-derived macrophages (BMDMs) and human MDMs, indicating that primary macrophages also utilize bidirectional TCA cycle metabolism to synthesize itaconate. Under hypoxic conditions, IDH-dependent reductive carboxylation predominated glutamine-dependent itaconate synthesis in all three kinds of macrophages. Similarly, inhibiting ETC activity with rotenone (complex I) or antimycin (complex III) abolished itaconate synthesis via oxidative TCA cycling in LPS-stimulated RAW 264.7 macrophages (Fig. 2E). Under conditions of impaired mitochondrial respiration (hypoxia or ETC inhibition), we observed reduced intracellular accumulation of itaconate M(LPS) RAW 264.7 macrophages and BMDMs (Fig. 2F). While the direct inhibition of ETC activity with antimycin depleted intracellular itaconate in hMDMs, we detected an unexpected increase of intracellular itaconate during the incubation of LPS-stimulated hMDMs at hypoxia (Fig. 2G). We speculated that species-specific metabolic reprogramming of pro-inflammatory macrophages underlies this drastic difference in hypoxic itaconate synthesis between human and murine macrophages [23].

In summary, we identified an unprecedented role of IDH-dependent reductive carboxylation in supporting de novo itaconate synthesis. Impairment in respiratory activity elevated the fractional contribution of reductive carboxylation to itaconate synthesis, while reducing the accumulation of itaconate in mouse macrophages. In contrast, hMDMs increased the accumulation of itaconate under hypoxic conditions, demonstrating an unusual high preference on reductive carboxylation for itaconate synthesis in human macrophages.

2.3. Itaconate attenuates the reductive carboxylation of α-KG to isocitrate or 2-hydroxyglutarate

M(LPS) macrophages switch from OXPHOS to aerobic glycolysis through a metabolic adaptation described as pseudohypoxia [17,24]. A key driver for this metabolic reprogramming is the transcription factor HIF-1-α and stabilization of HIF-1-α under hypoxic conditions has been shown to induce reductive carboxylation of α-KG to isocitrate through the reverse activity of IDH [14]. Within mitochondria this activity is catalyzed by IDH2 and required reducing equivalents are supplied by NADPH. Despite a stabilization of HIF-1-α in pro-inflammatory macrophages, an increase in reductive IDH activity has not been reported in previous studies [16,17,24]. Likewise, we did not observe an increase in reductive carboxylation activity in LPS-treated RAW 264.7 macrophages, contrary to hypoxic conditions, which strongly augmented reductive IDH flux (Fig. 3A).

We speculated that itaconate might limit the reductive activity of IDH, which we tested by incubating fractionated RAW 264.7 macrophage mitochondria in the presence of [U-^{13}C]-glutamine. Treatment of mitochondria with 10 mM itaconate induced a strong reduction in the ratio of M5 citrate to M5 α-KG (Fig. 3B). In addition, we determined the enrichment pattern of isocitrate, which was almost identical to that of citrate, proving evidence that itaconate inhibits reductive IDH2 and not ACO2 activity (Fig. 3B). We further evaluated the effect of itaconate on reductive carboxylation in primary macrophages and observed that itaconate inhibits IDH2 in mitochondria of hMDMs to a similar degree (Fig. 3C). This inhibition is furthermore not specific to macrophages, as 10 mM itaconate abolished reductive carboxylation in mitochondria of human intestinal epithelial HT29 cells and human adenocarcinomic alveolar A549 cells (Fig. 3D).

NADPH-dependent IDH1/2 has been shown to catalyze the reduction of α-KG to D-2-hydroxyglutarate (D-2-HG) at a low rate (Fig. 3E) and LPS or hypoxic conditions have been reported to increase the production of D-2-HG [25]. Specific IDH1 or IDH2 mutations potently elevate 2-HG production, leading to the inhibition of α-KG-dependent dioxygenases and driving tumor progression [26]. We observed strongly reduced levels of M5 2-HG in mitochondria of fractionated RAW 264.7 macrophages (Fig. 3F) or hMDMs (Fig. 3G) upon treatment with itaconate, demonstrating a reduced IDH2-dependent flux from α-KG to 2-HG.

2.4. Endogenous itaconate exerts feedback-inhibition on IDH2

We demonstrated that exogenous itaconate readily inhibits the reductive carboxylation of α-KG to isocitrate at IDH2 in fractionated mitochondria. To test whether endogenously synthesized itaconate is sufficient to attenuate reductive IDH2 activity, we incubated fractionated mitochondria from M(LPS) macrophages in the presence of [U-^{13}C]-glutamine and measured the ratio of reductive (M5) to oxidative (M4) citrate over the course of several time points (Fig. 4A). During 45 min of incubation, the fractional contribution of glutamine-derived carbon to citrate shifted from M5 citrate (reductive) to M4 citrate (oxidative), correlating with the accumulation of itaconate in the same time span (Fig. 1C), thus indicating that de novo produced itaconate limits the reductive activity of IDH2. To further validate this hypothesis we treated *Acod1* silenced RAW 264.7 macrophages with LPS in the presence of [U-^{13}C]-glutamine. The silencing of *Acod1* expression depleted cellular itaconate levels and increased reductive carboxylation in LPS-stimulated whole cell macrophages (Fig. 4B + C). Similarly, the inhibition of reductive carboxylation in mitochondria of LPS-stimulated macrophages was alleviated by the silencing of *Acod1* (Fig. 4D). These data provide evidence that endogenous itaconate is the primary driver of IDH2-inhibition during LPS stimulation, which we next set out to confirm in primary cells. As expected, we observed abolished cellular

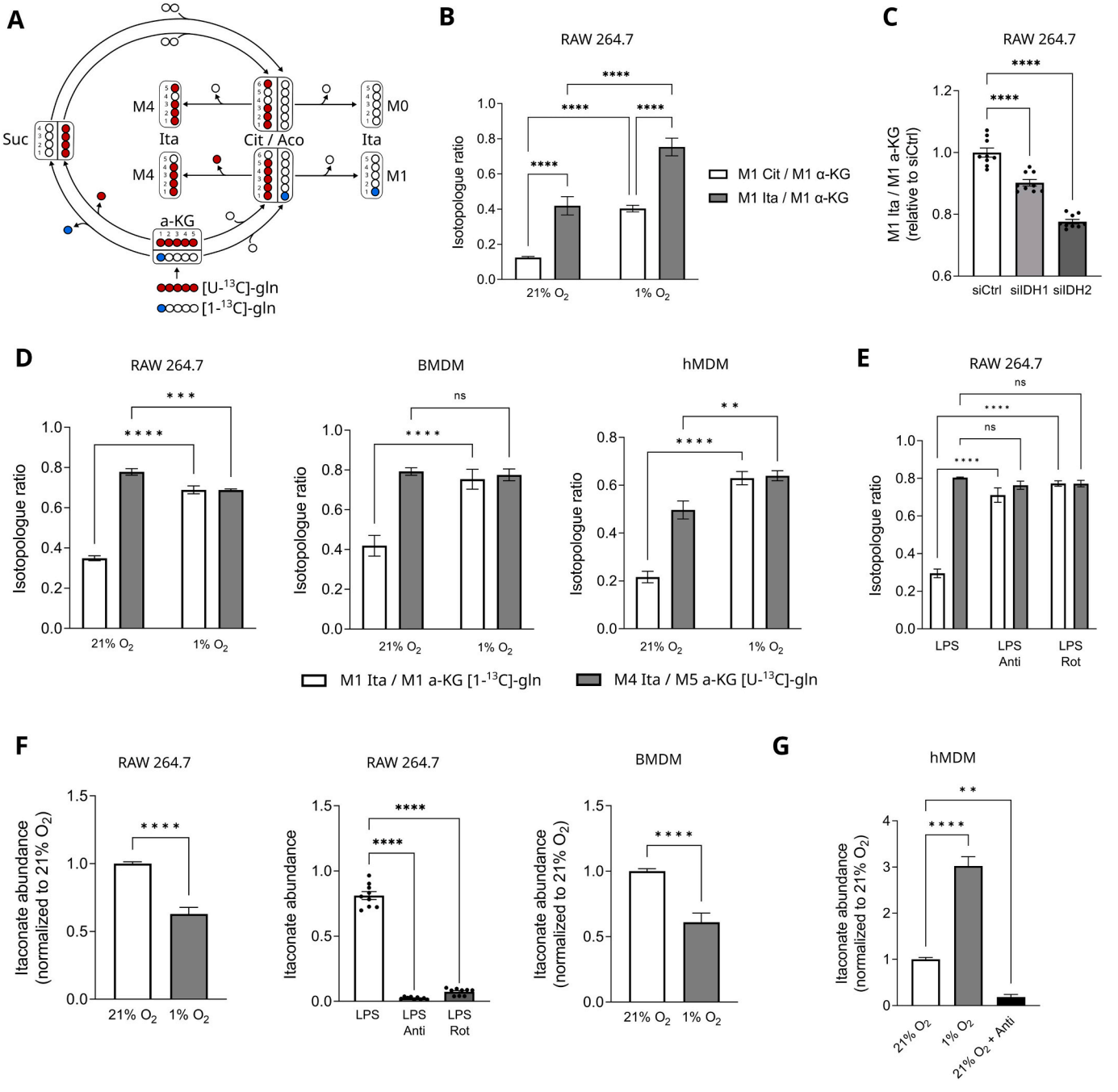

Fig. 2. Reductive carboxylation is a major pathway supplying carbon for itaconate synthesis. A. Atom transitions with [1-^{13}C]-glutamine (^{13}C carbon in blue) or [U—^{13}C]-glutamine (^{13}C carbon in red) showing that a combination of both tracers is needed to resolve the fractional contribution of glutamine to itaconate synthesis. B. Ratio of M1 citrate to M1 α-ketoglutarate (α-KG) or M1 itaconate to M1 α-KG in RAW 264.7 macrophages treated with 10 ng/ml LPS for 6 h at 1 % O_2 or 21 % O_2 levels in the presence of [1-^{13}C]-glutamine. C. Ratio of M1 itaconate to M1 α-KG in RAW 264.7 macrophages transfected with siRNA for isocitrate dehydrogenase 1 (IDH1) and 2 (IDH2) and stimulated with LPS for 6 h in the presence of [1-^{13}C]-glutamine. D,E. Ratios of M1 itaconate to M1 α-KG (reductive carboxylation of glutamine-derived carbon to itaconate) and M4 itaconate to M5 α-KG (flux of glutamine-derived carbon via both directions of the TCA cycle) in RAW 264.7 macrophages, human monocyte-derived macrophages (hMDMs), or mouse bone marrow-derived macrophages (BMDM) labeled with either [1-^{13}C]-glutamine or [U—^{13}C]-glutamine and treated with 10 ng/ml LPS for 6 h at 1 % O_2 or 21 % O_2 levels. RAW 264.7 macrophages were additionally treated with 2 μM antimycin A or rotenone for 6 h (E). F,G. Intracellular itaconate levels in RAW 264.7 macrophages, hMDMs or BMDMs treated with 10 ng/ml for 6 h at 1 % O_2 or 21 % O_2 levels. RAW 264.7 macrophages were additionally treated with 2 μM antimycin A or rotenone for 6 h at 21 % O_2 levels. All data are presented as mean ± SEM calculated from n = 3 replicates from 3 independent experiments. * $P < 0.05$, ** $P < 0.01$, *** $P < 0.001$, **** $P < 0.0001$ calculated by unpaired *t*-test (F), one-way ANOVA with Šidák post-test (B,C,G,H), or two-way ANOVA with Šidák post-test (D,E). (For interpretation of the references to colour in this figure legend, the reader is referred to the web version of this article.)

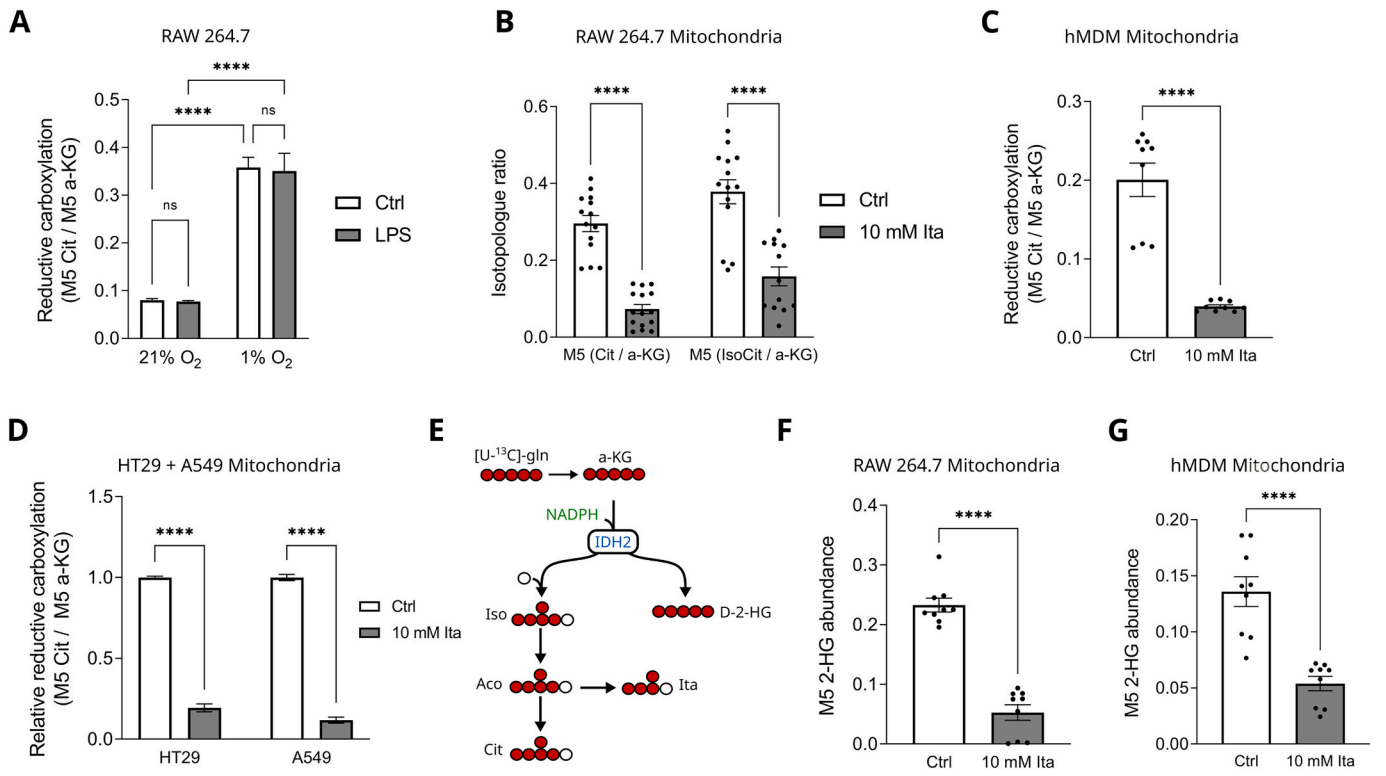

Fig. 3. Itaconate inhibits mitochondrial reductive carboxylation at IDH2. A. Reductive isocitrate dehydrogenase (IDH) flux in RAW 264.7 macrophages labeled with [U-^{13}C]-glutamine and stimulated with 10 ng/ml LPS for 6 h at 21 % O_2 or 1 % O_2 levels. B,C,D. Flux through IDH2 (M5 citrate/M5 α-ketoglutarate (α-KG)) or IDH2 and aconitase (M5 isocitrate/M5 α-KG) in fractionated mitochondria of RAW 264.7 macrophages (B), or human monocyte-derived macrophages (hMDMs) (C), or HT29 and A549 cells (D) treated with 10 mM itaconate for 30 min in the presence of [U-^{13}C]-glutamine. E. Atom transitions from [U—^{13}C]-glutamine tracer demonstrating production of D-2-hydroxyglutarate (2-HG) by IDH2. F,G. Ratio of M5 2-HG to M5 α-KG in mitochondria of RAW 264.7 macrophages (F), or hMDM (G) treated for 30 min with 10 mM itaconate in the presence of [U-^{13}C]-glutamine. All data are presented as mean ± SEM calculated from n = 3 replicates of 3 independent experiments. * $P < 0.05$, ** $P < 0.01$, *** $P < 0.001$, **** $P < 0.0001$ calculated by unpaired *t*-test (C,F,G) or one-way ANOVA with Šidák post-test (A), or two-way ANOVA with Šidák post-test (B,D).

itaconate synthesis (Supplement 1A), increased cellular reductive carboxylation (Supplement 1B) and increased mitochondrial reductive carboxylation (Supplement 1C) in *Acod1*-deficient BMDMs, indicating similar regulatory mechanisms of endogenous itaconate in primary cells.

Our results indicate that itaconate inhibits its own production pathway via feedback-inhibition. To further validate this hypothesis, we measured the fraction of IDH2-derived itaconate at different stages of activation by selectively treating RAW 264.7 macrophages with [U-^{13}C]-glutamine during the last 6 h of early (6 h) or late (22*h*) LPS stimulation. We hypothesized that accumulated itaconate during prolonged LPS stimulation augments the inhibition of IDH2, while low itaconate levels during early LPS stimulation allow for a high reductive flux through IDH2. In fact, we could observe a marked reduction in the ratio of reductive carboxylation-derived itaconate during the late window of LPS stimulation (Fig. 4E). We next inhibited NADPH-dependent IDH with oxalomalate to demonstrate how IDH2 inhibition affects itaconate synthesis. Treatment of LPS-stimulated RAW 264.7 macrophages with oxalomalate in the presence of [1-^{13}C]-glutamine potently inhibited reductive itaconate production, as the ratio of M1 itaconate to M1 α-KG was reduced (Fig. 4F). This correlated with lower itaconate levels, particularly under hypoxia, which is plausible because itaconate synthesis is heavily supplied by IDH-dependent reductive carboxylation under hypoxic conditions (Fig. 4G). We conclude that there is sufficient evidence supporting our hypothesis that itaconate limits the activity of its own production pathway via feedback-inhibition of IDH2.

2.5. Inhibition of IDH2 by itaconate is linked to alterations of mitochondrial redox metabolism

We next set out to understand the mechanism underlying the attenuation of reductive carboxylation by itaconate. We first hypothesized that a reductive IDH2 activity could be impaired by an increase in the mitochondrial ratio of citrate to α-KG (assuming that isocitrate and citrate are in equilibrium) (Fig. 5A). In line with previous studies [22], we could confirm that the complex I inhibitor rotenone decreases the ratio of citrate to α-KG in mitochondria of RAW 264.7 macrophages, correlating with a strong increase in reductive carboxylation (Figs. 5B and 6C). Despite the inhibition of reductive carboxylation by itaconate, we did not detect major changes in the ratio of citrate to α-KG in mitochondria of RAW 264.7 macrophages. Indeed, itaconate even further decreased the ratio of citrate to α-KG in rotenone-treated mitochondria, despite reducing the reductive activity of IDH.

Having established that the effect of itaconate on IDH2 is independent of the substrate/product ratio, we next considered a limited supply of the co-factor NADPH. We first measured the ratio of $NADP^+$ to NADPH in mitochondria of RAW 264.7 macrophages treated with itaconate for 30 min (Fig. 5D). Itaconate increased the ratio of $NADP^+$ to NADPH and could hereby limit the availability of NADPH for reductive carboxylation at IDH2. Previous studies also demonstrated a strong inhibitory effect of $NADP^+$ on IDH1, which might also apply for IDH2 because of the high structural similarity between these two isoforms [27]. Besides nicotinamide nucleotide transhydrogenase (NNT), a major source for mitochondrial NADPH production is malic enzyme (ME3) activity which relies on mitochondrial malate. We observed that itaconate, a competitive SDH inhibitor, reduced levels of malate in

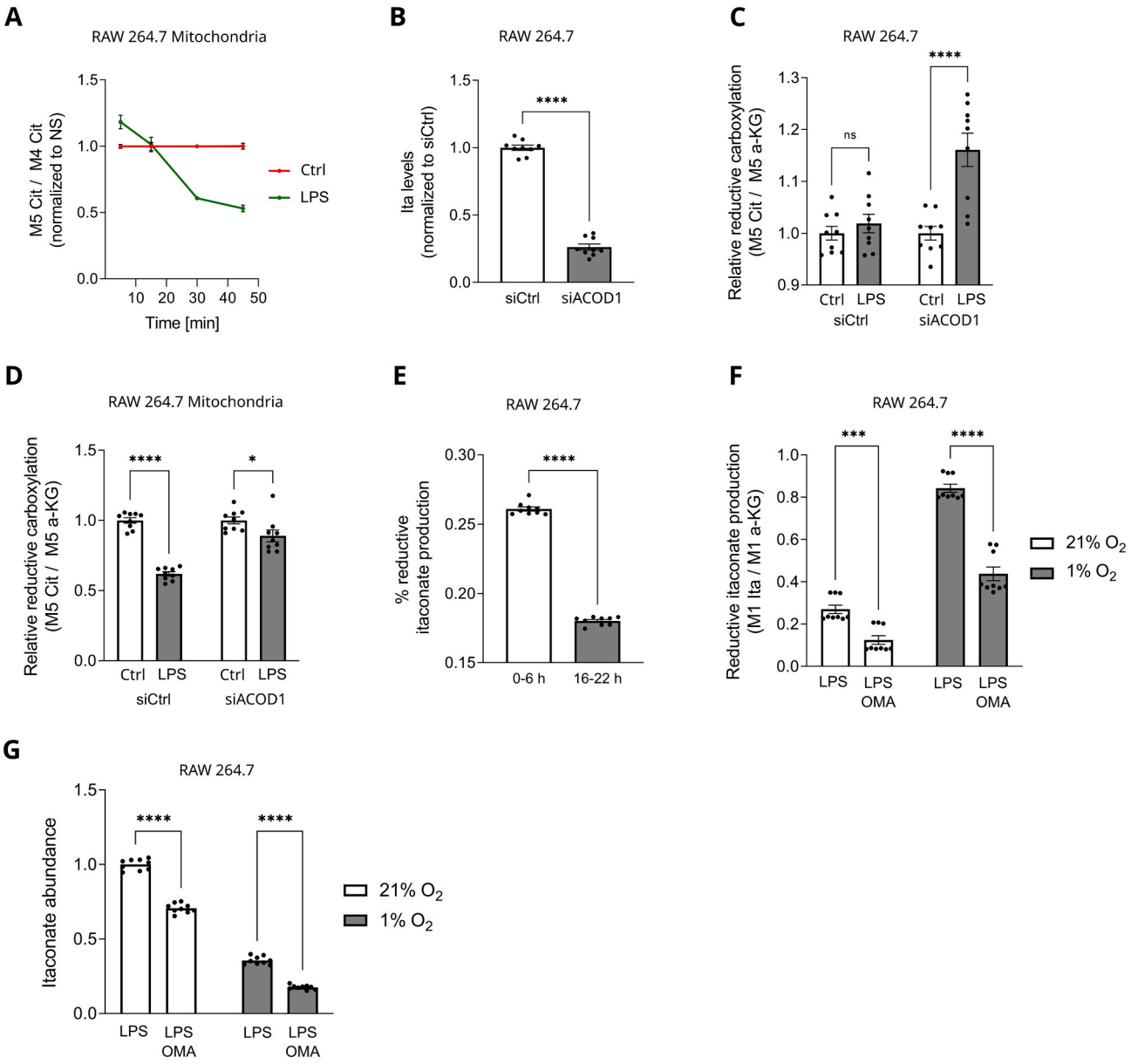

Fig. 4. Feedback-inhibition of IDH2 by itaconate. A. Relative ratio of M5 citrate to M4 citrate in mitochondria of LPS pre-stimulated RAW 264.7 macrophages treated for 5 to 45 min with [U-^{13}C]-glutamine. B,C,D. Relative intracellular itaconate levels (B), or relative reductive carboxylation activity (C,D) in RAW 264.7 macrophages (B,C), or mitochondria of RAW 264.7 macrophages (D) transfected with siRNA for *Acod1* or non-specific siRNA and stimulated with 10 ng/ml LPS for 6 h. E. Percentage of itaconate produced via reductive carboxylation in RAW 264.7 macrophages stimulated with LPS for 6 or 22 h and treated with [U-^{13}C]-glutamine and [1-^{13}C]-glutamine for the last 6 h of incubation. F,G. Itaconate abundance (F), or activity of IDH-dependent itaconate production (G) in RAW 264.7 macrophages pretreated with 1 mM oxalomalate (OMA) for 1 h, followed by stimulation with 10 ng/ml LPS for 6 h at 21 % O_2 or 1 % O_2. All data are presented as mean ± SEM calculated from n = 3 replicates of 3 independent experiments. * $P < 0.05$, ** $P < 0.01$, *** $P < 0.001$, **** $P < 0.0001$ calculated by unpaired *t*-test (B,E) or two-way ANOVA with Šidák post-test (C,D,F,G).

mitochondria of RAW 264.7 macrophages (Fig. 5E). Additionally, we observed a reduced ratio of M3 pyruvate to M4 malate in mitochondria labeled with [U-^{13}C]-glutamine, indicative of an attenuated ME3 activity (Fig. 5F). Consistent with the correlation between the activity of SDH, ME3 and reductive carboxylation, we detected that mitochondria treated with the itaconate isomer mesaconate, which exerts a much weaker inhibitory effect on SDH, maintain reductive carboxylation activity (Fig. 5G). We next sought to rescue ME3 activity by supplementing fractionated mitochondria with malate, but detected only a minor increase in reductive carboxylation activity not fully explaining the observed inhibition of reductive carboxylation (Fig. 5H). Furthermore, we could rule out SDH inhibition as the primary mechanism underlying the attenuation of reductive carboxylation by itaconate. After treating mitochondria with the irreversible SDH inhibitor 3-NPA, we did not observe a decreased reductive activity of IDH2 in mitochondria of RAW 264.7 macrophages, but indeed additional treatment with itaconate depleted reductive carboxylation (Fig. 5I). In line, 3-NPA and mesaconate also did not increase the mitochondrial ratio of $NADP^+$ to NADPH (Fig. 5J). We therefore conclude that the inhibition of IDH2 by itaconate is linked to alterations of the mitochondrial redox balance, competitive SDH inhibition and ME3 inhibition.

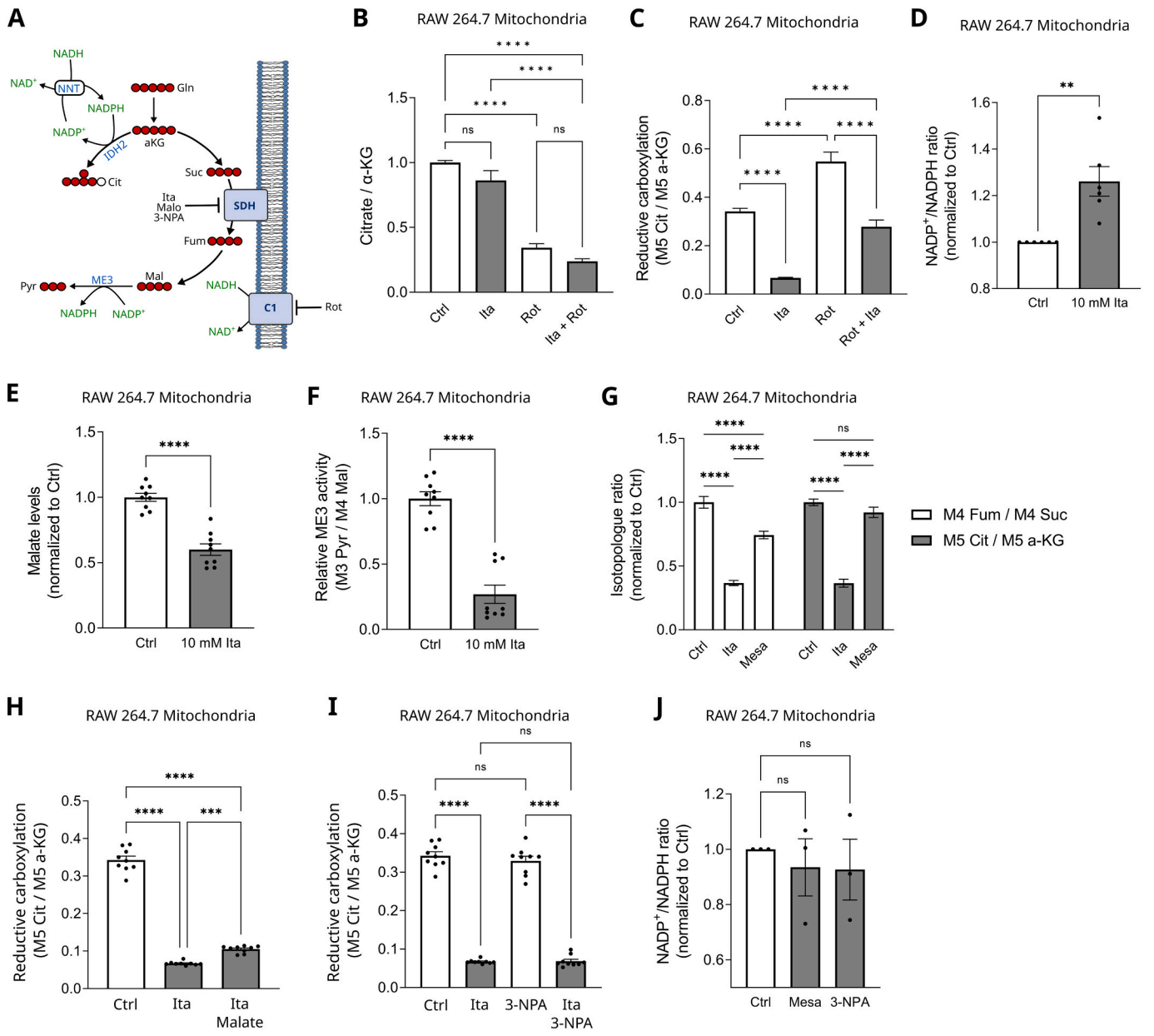

Fig. 5. Inhibition of IDH2 by itaconate linked to changes in mitochondrial metabolism. A. Atom transitions from [U—^{13}C]-glutamine tracer showing selected reactions involved in mitochondrial redox homeostasis. B,C. Ratio of citrate to α-KG metabolite levels (B), or ratio of M5 citrate to M5 α-ketoglutarate (α-KG) (C) in mitochondria of RAW 264.7 macrophages treated with 10 mM itaconate or 2 μM rotenone (rot) for 30 min in the presence of [U-^{13}C]-glutamine. D,E,F. Relative ratio of $NADP^+$ to NADPH (D), or malate levels (E), or relative ratio of M3 pyruvate to M4 malate (F) in mitochondria of RAW 264.7 macrophages treated with 10 mM itaconate for 30 min. G. Relative ratio of M4 fumarate to M4 succinate, or M5 citrate to M5 α-KG in mitochondria of RAW 264.7 macrophages treated with 10 mM itaconate or 10 mM mesaconate for 30 min in the presence of [U-^{13}C]-glutamine. H,I. Ratio of M5 citrate to M5 α-KG in mitochondria of RAW 264.7 macrophages treated with 10 mM itaconate and 1 mM malate (H), or 0.1 mM 3-NPA (I) for 30 min in the presence of [U-^{13}C]-glutamine. J. Relative ratio $NADP^+$ to NADPH in mitochondria of RAW 264.7 macrophages treated with 10 mM mesaconate or 0.1 mM 3-nitropropionate (3-NPA) for 30 min. All data are presented as mean ± SEM calculated from n = 3 replicates of 3 independent experiments, or (D) n = 3–6 replicates from 6 independent experiments. * $P < 0.05$, ** $P < 0.01$, *** $P < 0.001$, **** $P < 0.0001$ calculated by unpaired t-test (D,E,F) or two-way ANOVA with Šidák post-test (B,C,G,H,I,J).

2.6. Cell type-specific reprogramming of mitochondrial metabolism in a time- and dose-dependent manner

To obtain a more comprehensive overview of cell type-specific itaconate synthesis in activated macrophages and evaluate how reductive carboxylation activity is regulated in different types of macrophages, we next analyzed the effect of time- (6 h vs. 24 h) and dose- (10 ng/ml vs. 1000 ng/ml LPS) effects on the flux of carbon from glucose, glutamine and palmitate into the TCA cycle of RAW 264.7 macrophages, BMDMs and hMDMs (Fig. 6A). Besides the synthesis of itaconate with glutamine-derived α-KG via aforementioned decarboxylation/carboxylation pathways, we observed that itaconate is furthermore supplied by second-round oxidative TCA cycling (M2 itaconate [U—^{13}C]-glutamine), second-round reductive carboxylation (M3 itaconate [U—^{13}C]-glutamine), as well as the carboxylation of glucose-derived pyruvate (M3 and M4 itaconate [U—^{13}C]-glucose) (Fig. 6A,B). Oxidation of [U-^{13}C]-palmitate did not fuel the synthesis of itaconate in RAW 264.7 macrophages, but we observed a minor contribution of palmitate-derived carbon to the labeling of itaconate in BMDMs and hMDMs. The metabolic response of the three types of macrophages to the time

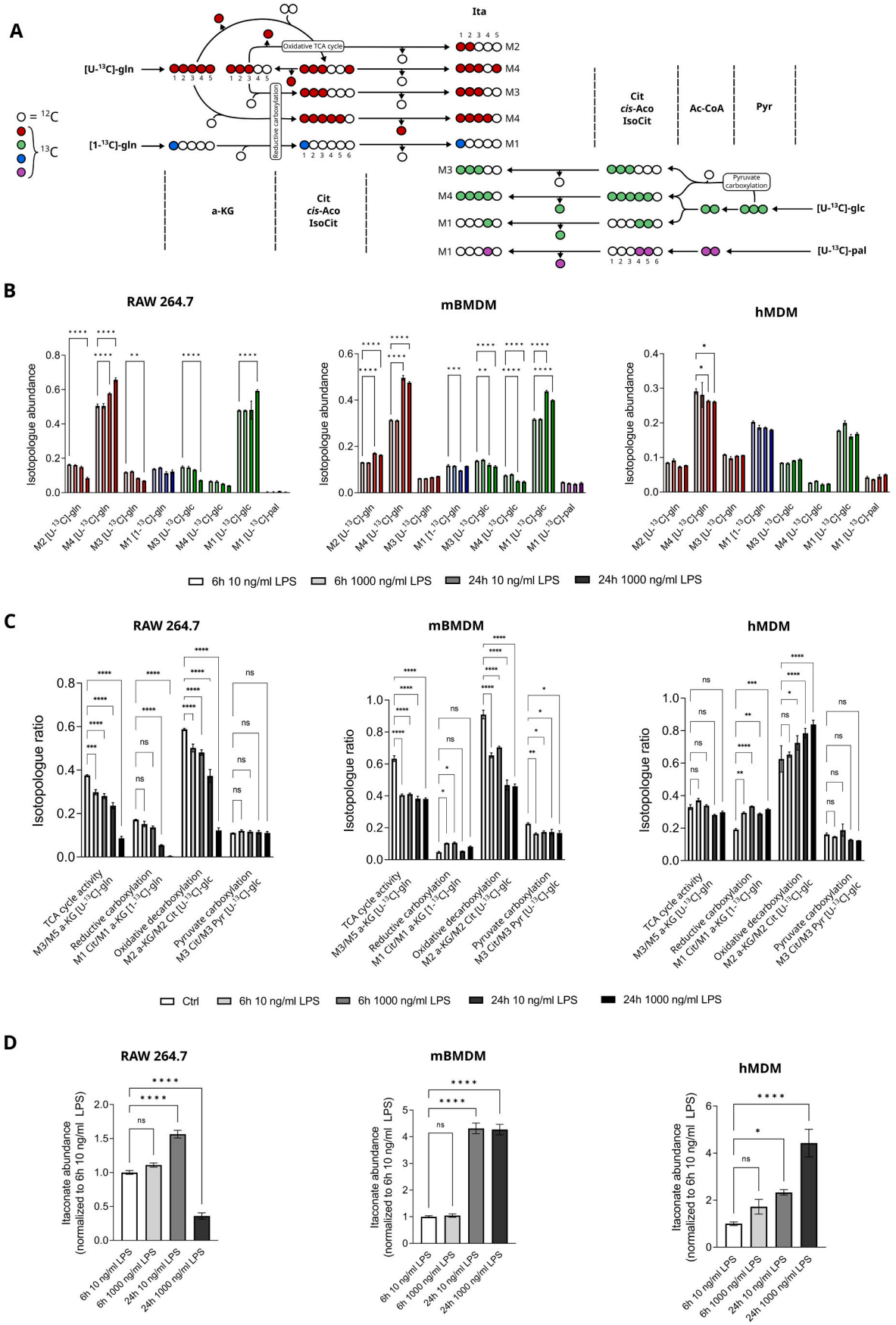

(caption on next page)

Fig. 6. Time-, dose- and cell type-specific TCA cycle fluxes and itaconate production. A. Atom transitions in TCA cycle from [U—^{13}C]-glutamine (red circles), [1-^{13}C]-glutamine (blue circles), [U—^{13}C]-glucose (green circles) and [U-^{13}C]-palmitate (violet circles) showing the metabolic origin of different itaconate isotopologues. B. Fractional abundance of selected itaconate isotopologues in RAW 264.7 macrophages, human monocyte-derived macrophages (hMDMs), or mouse bone marrow-derived macrophages (BMDM) labeled with [U-^{13}C]-glutamine (red), [1-^{13}C]-glutamine (blue), [U—^{13}C]-glucose (green) or [U—^{13}C]-palmitate (violet) for 24 h in the presence of 10 or 1000 ng/ml LPS for 6 or 24 h. C. TCA cycle activity (M3 α-ketoglutarate (α-KG) divided by M5 α-KG in cells labeled with [U-^{13}C]-glutamine), reductive carboxylation activity (M1 citrate divided by M1 α-KG in cells labeled with [1-^{13}C]-glutamine), oxidative IDH activity (M2 α-KG divided by M2 citrate in cells labeled with [U-^{13}C]-glucose) and rate of pyruvate carboxylation (M3 citrate divided by M3 pyruvate in cells labeled with [U-^{13}C]-glucose) in RAW 264.7 macrophages, BMDMs and hMDMs treated with 10 or 1000 ng/ml LPS for 6 h or 24 h. D. Relative itaconate levels in RAW 264.7 macrophages, BMDMs and hMDMs treated with 10 or 1000 ng/ml LPS for 6 h or 24 h. All data are presented as mean ± SEM calculated from n = 3 replicates from 3 independent experiments (RAW 264.7), or n = 3 replicates from 2 independent experiments (BMDMs), or 1 representative experiment out of two independent experiments with n = 3 replicates (hMDMs). * $P < 0.05$, ** $P < 0.01$, *** $P < 0.001$, **** $P < 0.0001$ calculated by one-way ANOVA with Šidák post-test (D), or two-way ANOVA with Šidák post-test (B,C). (For interpretation of the references to colour in this figure legend, the reader is referred to the web version of this article.)

and dose of LPS-stimulation was highly distinct (Fig. 6B,D). RAW 264.7 macrophages decreased oxidative TCA cycling, as well as the oxidative activity of IDH, in a time- and LPS dose-dependent manner. Expectedly, we observed a drastic reduction of reductive carboxylation activity in LPS-stimulated RAW 264.7 macrophages, indicating that the inhibition of reductive IDH activity precedes the shut-down of oxidative TCA cycle activity. The bidirectional break between citrate and α-KG correlated with depleted itaconate levels in RAW 264.7 macrophages treated with 1000 ng/ml LPS for 24 h (Fig. 6D), indicating that an inhibition of bidirectional TCA cycling limits further de novo itaconate synthesis under these conditions.

While we observed a similar inhibitory trend of prolonged LPS stimulation on oxidative and reductive IDH activity in BMDMs and RAW 264.7 macrophages, LPS-stimulated BMDMs maintained a higher degree of bidirectional TCA cycling after 24 h of LPS-stimulation, correlating with high intracellular itaconate levels under these conditions. Contrary to RAW 264.7 macrophages, BMDMs augmented the reductive carboxylation activity of IDH during early LPS stimulation. As a previous study identified a shut-down of oxidative TCA cycling and itaconate synthesis between 24 and 48 h of LPS and IFN-γ stimulation, we conclude that LPS-stimulated RAW 264.7 macrophages decrease mitochondrial TCA cycle activity more rapidly than BMDMs [12]. Intriguingly, we could not detect notable differences in the metabolic response of BMDMs with regard to different LPS doses, indicating that 10 ng/ml LPS are sufficient to fully stimulate metabolic reprogramming in BMDMs (Fig. 6C,D).

Contrary to mouse macrophages, we found that LPS-stimulated hMDMs augmented the reductive and oxidative activity of IDH over time. These findings align with a previously published study, which demonstrated that hMDMs, but not BMDMs, maintain a high rate of mitochondrial respiration during prolonged LPS stimulation [23]. Expectedly, the accumulation of itaconate correlated with increased time and dose of LPS treatment. LPS-stimulated hMDMs were capable of maintaining a high reductive carboxylation activity, potentially due to comparatively low intracellular itaconate levels and thus a lower inhibitory effect on reductive IDH activity [3].

Taken together, our findings exhibit distinct regulation of itaconate synthesis and TCA cycle metabolism in different types of LPS-stimulated macrophages. RAW 264.7 macrophages are highly susceptible to increased LPS concentrations and shut down bidirectional TCA cycling and itaconate production already after 24 h of stimulation. Mouse BMDMs are metabolically less responsive to elevated LPS concentrations and maintain a higher degree of bidirectional TCA cycling and itaconate during the first 24 h of LPS treatment. In contrast to mouse macrophages, human MDMs increase bidirectional IDH activity and itaconate synthesis in a dose- and time-dependent way.

3. Discussion

An ever-growing number of findings in the last decade have highlighted the crucial role of metabolic reprogramming for macrophage function [1]. In this study we aimed to extend the canonical model TCA cycle reprogramming in M(LPS) macrophages by investigating the relationship between itaconate and mitochondrial metabolism. Using stable-isotope tracing in fractionated mitochondria, we first established that itaconate is in fact produced inside mitochondria of activated macrophages. De novo synthesized itaconate inhibits SDH, however it does not induce a quantitative break in oxidative TCA cycling at early time-points post LPS stimulation, indicating that the attenuation of the oxidative TCA cycle flux in activated macrophages is to a major extent independent of itaconate.

The reductive carboxylation of α-KG to isocitrate has been generally deemed insignificant in M(LPS) macrophages as multiple studies demonstrated a low fractional contribution of M5 citrate to the pool of labeled citrate in LPS-stimulated macrophages labeled with [U-^{13}C]-glutamine [12,16]. We demonstrate that this is the case because reductive carboxylation-derived carbon is preferably rerouted to itaconate by ACOD1. Given the fact that itaconate can accumulate inside macrophages up to millimolar concentrations, the reductive flux through IDH must be considerable. In fact, during partial inhibition of mitochondrial respiration at hypoxic conditions, glutamine-derived itaconate was almost exclusively produced via reductive carboxylation. As physiological tissue oxygen levels are expected to be in a range of 1 % to 9 % [20], depending on the tissue and pathophysiological context [28], it is very likely that reductive carboxylation through IDH is an important pathway for itaconate synthesis in vivo. As we obtained a comparable fractional contribution reductive carboxylation to itaconate synthesis in primary human and mouse macrophages, it appears that a high reductive flux through IDH is not a consequence of cancer metabolism. In mouse macrophages, inhibiting oxidative TCA cycle metabolism (hypoxia, ETC inhibitors, prolonged LPS stimulation) and reductive carboxylation (oxalomalate) depleted intracellular itaconate, indicating that M(LPS) macrophages rely on bidirectional TCA cycle metabolism to sustain maximal itaconate production. This concept fits to previously published results, which demonstrated that oxidation of glutamine-derived carbon and concomitant production of NADH are required to sustain reductive carboxylation activity at IDH in respiration-deficient cells [29].

Despite a similar contribution of carbon sources and metabolic pathways to synthesize itaconate, we detected profound metabolic differences between RAW 264.7 macrophages and BMDMs with regard to the time and dose of LPS treatment. LPS-induced metabolic reprogramming in mouse and human macrophages was also highly contrasting. Contrary to BMDMs and RAW 264.7 macrophages, LPS-stimulated hMDMs augmented itaconate synthesis under hypoxic conditions. Previous publications showed that similar concentrations of LPS induce two orders of magnitude lower itaconate levels in human than in mouse macrophages [3]. According to our knowledge, a definitive reason for the observed difference in itaconate accumulation between human and murine macrophages has not been presented yet. We discern that human macrophages, contrary to mouse macrophages, maintain a high degree of oxidative TCA cycling during prolonged LPS stimulation. This is consistent with another study [23], that hMDMs do not switch from mitochondrial respiration to aerobic glycolysis. This indicates that hMDMs prioritize oxidative TCA cycling to sustain respiration over itaconate production. In fact, hypoxic conditions recapitulate aspects of LPS-induced pseudohypoxia, which potentially enables the increased

redirection of carbon towards itaconate synthesis.

Macrophages potently downregulate the expression of $NADP^+$-dependent *Idh1* and *Idh2* [12]. We further identified that itaconate itself attenuates the activity of IDH2 by inhibiting reductive carboxylation. We speculate that reductive IDH activity is especially utilized during early LPS stimulation to quickly generate high amounts of itaconate through bidirectional TCA cycle metabolism. In a later stage of LPS stimulation, reductive carboxylation is gradually attenuated by the accumulated itaconate, which in turn restricts further itaconate accumulation, exhibiting a negative feedback on itaconate production. This is in line with the reported dynamics of itaconate production in LPS-stimulated macrophages [10,12]. As itaconate has been identified as a key mediator of endotoxin tolerance in monocytes and macrophages [30,31], reductive carboxylation and IDH2 might emerge as novel regulators during immune tolerance. Indeed, our preliminary results showed that inhibition of reductive carboxylation by oxalomalate under hypoxic conditions not only reduced itaconate production, but also increased cytokine expression in re-stimulated tolerized macrophages. This warrants further investigation to verify such regulation in a pathological context.

Inhibition of SDH by itaconate increases superoxide formation by promoting reverse electron transport to complex I [32], which might increase NADPH-dependent production of reduced glutathione as antioxidant, driving the need to modulate NADPH-consuming pathways. Recently, the accumulation of the oncometabolite 2-HG has been reported in activated macrophages [25]. We speculate that this might be a direct consequence of a high reductive IDH activity, which catalyzes the reduction of α-KG to 2-HG at a low rate. Expectedly, itaconate also inhibits IDH2-dependent production of 2-HG. A recent study further identified that D-2-HG (IDH-derived enantiomer) accumulates in human and mouse macrophages during the late window of LPS stimulation (24 h) and this increase might be mediated by hydroxyacid-oxacid transhydrogenase (HOT), a 2-HG-producing enzyme induced during LPS stimulation [33]. While in our study, we only looked at the effect of itaconate on 2-HG production during the early window of LPS stimulation and with regard to IDH2. The potential of itaconate to control signaling and oncogenic properties of 2-HG during prolonged LPS treatment warrants further investigation. Mechanistically, we showed that inhibition of IDH2 by itaconate is associated with a shift towards $NADP^+$ accumulation in macrophage mitochondria, which is not shared by the itaconate isomer mesaconate, or the non-competitive SDH inhibitor 3-NPA. As we did not observe notable changes of the substrate/product ratio of IDH2 during itaconate treatment on mitochondria, it is likely that alterations of the mitochondrial co-factor balance regulate IDH2 activity. The yet-unknown basis underlying the itaconate-induced shift in the mitochondrial $NADPH/NADP^+$ ratio awaits further investigation. Our findings further indicate that itaconate does not inhibit IDH2 directly. However, based on our current findings, we cannot rule out additional mechanisms of IDH2 inhibition by itaconate, like affecting post-translational acetylation or succinylation, which have been reported to potently affect IDH2 activity [34,35].

To sum up, our findings provide now insights into TCA cycle reprogramming during pro-inflammatory macrophage activation and identify mitochondrial redox dynamics as a crucial determinant and potential intervention target to the function of inflammatory macrophages.

4. Material and methods

4.1. Cell culture

Mouse macrophage RAW 264.7 cells (Sigma-Aldrich, Steinheim, Germany), human pulmonary carcinoma epithelial A549 cells and human colon epithelial HT29 cells were cultured in DMEM5030 medium (Gibco, 41965039) containing 10 % heat-inactivated FBS (Gibco, A3840401) and 1 % (v/v) penicillin/streptomycine in a humidified incubator at 5 % CO_2. BMDMs were derived from bone marrow isolated from the tibia of C57BL/6 J mice and differentiated in DMEM5030 medium containing 10 % heat-inactivated FBS, 1 % (v/v) penicillin/streptomycine and 25 ng/ml M-CSF (Miltenyi, Bergisch Gladbach, Germany) for 7 days. C57/B6 mice were maintained in the SPF facility of the University of Luxembourg in accordance with animal guidelines from local and university authorities, under specific pathogen-free condition. Human monocyte-derived macrophages were isolated from buffy coats utilizing Biocoll (Bio&Sell, Feucht, Germany) and CD14 microbeads (Miltenyi, Bergisch Gladbach, Germany). After informed consent, obtained blood samples were collected according to the guidelines of the local ethic committees and the guidelines of the World Medical Association Declaration of Helsinki. HMDMs were differentiated in RPMI1460 medium containing 50 U/ml M-CSF (ImmunoTool, Friesoythe, Germany) for 6–7 days.

4.2. Analysis of metabolites from whole cells and stable isotope tracing

RAW 264.7 macrophages were seeded in 12-well plates at 1 × 10ˆ5 cells per well. BMDM and hMDM cells were seeded in 12-well plates at 1 × 10ˆ6 cells per well. For experiments at hypoxia, cells were put into a humidified hypoxia chamber set to 1 % O_2 and 5 % CO_2 (Coy Laboratory Products, Grass Lake, USA) 20–24 h after seeding (RAW 264.7), or 4 h after seeding (BMDM, hMDM) and incubated for another 18 h. Approximately 36 h after seeding (RAW 264.7), or 22 h after seeding (BMDM, hMDM), the medium was replaced by DMEM medium containing the respective stable-isotope tracer instead of its unlabeled variant and dialyzed FBS. Cells were cultured with either 4 mM [U—^{13}C]-glutamine (all tracers: Cambridge Isotope Laboratories, USA), 4 mM [1-^{13}C]-glutamine, 25 mM [U—^{13}C]-glucose or 50 μM [U—^{13}C]-palmitate (conjugated to BSA as described previously [36]. Following tracer application, cells were treated with the indicated concentration of LPS for 6–24 h, after which metabolites were extracted as described below.

4.3. Analysis of metabolites from permeabilized cells

RAW 264.7 cells, A549 cells and HT29 cells were seeded in 6-well plates at 2.5 × 10ˆ5 cells per well and incubated for 44–48 h. BMDM and hMDM cells were seeded in 6-well plates at 2.5 × 10ˆ6 cells per well and incubated for 20–24 h. Permeabilization and assessment of mitochondrial metabolism was performed as published previously [21]. Briefly, cells were washed with PBS and selective permeabilization of the cytosolic membrane was induced by the addition of 40 μM digitonin for 2 min. After three consecutive washing steps in mitochondria buffer (2 mM KH_2PO_4, 120 mM KCl, 3 mM HEPES, 1 mM EGTA, 3 g/l essentially fatty-acid free BSA, pH 7.2), a combination of substrates (1 mM pyruvate and 1 mM glutamine) was added to the in situ mitochondria. After incubation for 5–45 min, mitochondria metabolites were extracted as described below.

4.4. Metabolite extraction and GC–MS measurement

Metabolites were extracted from complete and permeabilized cells as previously described [21]. Briefly, cells were washed with 0.9 % NaCl and quenched with ice-cold methanol and ice-cold ddH_2O (containing 1 μg/ml D6-glutaric acid as internal standard). Cells were scraped and cell extracts were added into tubes containing ice-cold chloroform. The extracts were vortexted at 1400 rpm for 20 min at 4 °C and centrifuged at 17000 *g* for 5 min at 4 °C to achieve phase separation. 300 μl of the upper polar phase were transferred into GC glass vials with microinsert and dried under vacuum at 4 °C. GC–MS measurement of relative metabolite levels and isotopic enrichment was performed as previously published. Dried extracts were derivatized using equal amounts of methoxylamine (20 mg/ml in pyridine) and MTBSTFA and injected into the GC–MS system. Metabolite separation was performed by an Agilent 7890B gas

chromatograph equipped with a 30 m DB-35 ms and 5 m Duruguard capillary column. Metabolites were detected in either full scan or selected ion mode by an Agilent 5977 MSD system. Analysis of chromatograms, calculation of mass isotopomer distributions and relative comparison of metabolites were carried out using the Metabolite Detector software [37].

4.5. siRNA-mediated gene silencing

The 4D nucleofector™ and SF Cell Line 4D-Nucleofector™ X kit (Lonza, Basel, Switzerland) were used to electroporate RAW 264.7 cells. Silencing was performed by ON-TARGETplus SMARTpool™ siRNAs for mouse *Irg1, Idh1* or *Idh2. s*iRNA ON-TARGET plus non-targeting pool was used as the control (siCtrl). Transfected cells were seeded in 12-well plates or 6-well plates a 5 × 10ˆ5 cells/well and incubated for 18 before stimulating with LPS for 6 h.

4.6. Measurement of mitochondrial $NADP^+$ and NADPH levels

Selective permeabilization of RAW 264.7 was performed as described before. After the incubation of fractionated mitochondria for 30 min with the compounds of interest, relative $NADP^+$ and NADPH levels were measured using the NADP/NADPH-Glo™ assay (Promega). The reaction mix and selective destruction of oxidized NADP was performed according to the manufacturer's instructions. Samples were incubated for 60 min and luminescence was measured in white 96 well plates.

4.7. Western blot analysis

For the generation of compartment-specific protein samples, 2 × 10ˆ6 RAW 264.7 macrophages were seeded in a 10 cm dish and incubated for 48 h. During the last 6 h, cells were stimulated with 10 ng/ml LPS or a vehicle control. The cells were washed with PBS and cytosolic proteins were liberated by adding 1.5 ml of a 40 μM digitonin solution in mitochondria buffer. After 3 washing steps with mitochondria buffer, mitochondrial proteins were extracted by adding 1.5 ml M-PER (Thermo Fisher Scientific) and scraping. Proteins from full cells were extracted by adding 1.5 ml M-PER directly after washing the cells with PBS once. Immunoblotting was performed as described in a previous publication [38]. The anti-*Irg1* antibody was purchased from Sigma-Aldrich.

4.8. Live/dead cell staining

The appropriate concentration of digitonin needed to achieve complete permeabilization while still maintaining mitochondrial activity of RAW 264.7 macrophages was determined by LIVE/DEAD viability staining (Invitrogen), as described previously [21], using 4 μM ethidium-homodimer 1 and 2 μM calcein-AM. A digitonin concentration of 40 μg/ml was selected for all further experiments, since it was the lowest dose which induced uniform permeabilization of the whole culture.

4.9. Statistical analysis

All values were presented as means ± SEM. Group comparison was performed by unpaired Students *t*-test (two groups), one-way or two-way ANOVA (for multiple groups) with Šidák multiple comparison test as noted in the figure legends. P values below $p < 0.05$ were considered statistically significant. Analysis and visualization were performed with Prism 9.0 (GraphPad) or LibreOffice.

Supplementary data to this article can be found online at https://doi.org/10.1016/j.bbadis.2022.166530.

Declaration of competing interest

The authors declare that they have no known competing financial interests or personal relationships that could have appeared to influence the work reported in this paper.

Data availability

Data will be made available on request.

Acknowledgments

The authors want to thank Sabine Kaltenhäuser for technical assistance and Prof. Thekla Cordes for helpful discussion.

CRediT authorship contribution statement

Alexander Heinz: Conceptualization, Methodology, Writing – original draft, Investigation, Formal analysis. **Yannic Nonnenmacher:** Conceptualization, Methodology, Writing – original draft, Investigation, Formal analysis. **Antonia Henne:** Investigation. **Michelle-Amirah Khalil:** Investigation. **Ketlin Bejkollari**: Investigation. **Catherine Dostert**: Investigation, Resources. **Shirin Hosseini**: Investigation. **Oliver Goldmann:** Resources. **Wei He**: Investigation, Writing – Review & Editing. **Roberta Palorini:** Methodology, Investigation. **Charlène Verschueren**: Investigation. **Martin Korte**: Resources, Writing – Review & Editing. **Ferdinando Chiaradonna**: Methology, Writing – Review & Editing. **Eva Medina**: Resources, Writing – Review & Editing. **Dirk Brenner:** Resources, Writing – Review & Editing. **Karsten Hiller:** Conceptualization, Writing – Review & Editing, Supervision.

Funding

This work was funded by the Federal State of Lower Saxony, Niedersächsisches Vorab (VWZN3266), (KH), Deutsche Forschungsgemeinschaft (DFG, German Research Foundation) project HI1400/3-1, (KH), SFB-1454 project number 432325352 (KH). DB is supported by the Fonds National de la Recherche Luxembourg (FNR), FNR-ATTRACT program (A14/BM/7632103), and by the FNR-CORE (C18/BM/12691266). DB and CD receive funding through the FNRS-Televie program (No. 7.4597.19).

References

[1] W. He, A. Heinz, D. Jahn, K. Hiller, Complexity of macrophage metabolism in infection, Current Opinion in Biotechnology 68 (2021) 231–239. Elsevier Ltd.
[2] L.A.J. O'Neill, A broken Krebs cycle in macrophages, Immunity 42 (3) (2015 Mar 17) 393–394.
[3] A. Michelucci, T. Cordes, J. Ghelfi, A. Pailot, N. Reiling, O. Goldmann, et al., Immune-responsive gene 1 protein links metabolism to immunity by catalyzing itaconic acid production, Proc. Natl. Acad. Sci. U. S. A. 110 (19) (2013) 7820–7825.
[4] D. Duncan, A. Lupien, M.A. Behr, K. Auclair, Effect of ph on the antimicrobial activity of the macrophage metabolite itaconate, Microbiology (United Kingdom) 167 (2021).
[5] V. Lampropoulou, A. Sergushichev, M. Bambouskova, S. Nair, E.E. Vincent, E. Loginicheva, et al., Itaconate links inhibition of succinate dehydrogenase with macrophage metabolic remodeling and regulation of inflammation, Cell Metab. 24 (2016) 158–166.
[6] M. Bambouskova, L. Gorvel, V. Lampropoulou, A. Sergushichev, E. Loginicheva, K. Johnson, et al., Electrophilic properties of itaconate and derivatives regulate the IκBζ-ATF3 inflammatory axis, Nature 556 (2018) 501–504.
[7] E.L. Mills, D.G. Ryan, H.A. Prag, D. Dikovskaya, D. Menon, Z. Zaslona, et al., Itaconate is an anti-inflammatory metabolite that activates Nrf2 via alkylation of KEAP1, Nature 556 (7699) (2018 Apr) 113–117.
[8] S.T. Liao, C. Han, D.Q. Xu, X.W. Fu, J.S. Wang, L.Y. Kong, 4-Octyl itaconate inhibits aerobic glycolysis by targeting GAPDH to exert anti-inflammatory effects, NatureCommunications 10 (2019) 1–11.
[9] A. Swain, M. Bambouskova, H. Kim, P.S. Andhey, D. Duncan, K. Auclair, et al., Comparative evaluation of itaconate and its derivatives reveals divergent inflammasome and type I interferon regulation in macrophages, NatureMetabolism 2 (2020) 594–602.

[10] W. He, A. Henne, M. Lauterbach, E. Geißmar, F. Nikolka, C. Koh, et al., Mesaconate is synthesized from itaconate and exerts immunomodulatory effects in macrophages, Nature Metabolism 4 (2022) 524–533.
[11] A.K. Jha, S.C.C.C. Huang, A. Sergushichev, V. Lampropoulou, Y. Ivanova, E. Loginicheva, et al., Network integration of parallel metabolic and transcriptional data reveals metabolic modules that regulate macrophage polarization, Immunity 42 (3) (2015 Mar 17) 419–430.
[12] G.L. Seim, E.C. Britt, S.V. John, F.J. Yeo, A.R. Johnson, R.S. Eisenstein, et al., Two-stage metabolic remodelling in macrophages in response to lipopolysaccharide and interferon-γ stimulation, Nat. Metab. 1 (2019) 731.
[13] E.M. Palmieri, M. Gonzalez-Cotto, W.A. Baseler, L.C. Davies, B. Ghesquière, N. Maio, et al., Nitric oxide orchestrates metabolic rewiring in M1 macrophages by targeting aconitase 2 and pyruvate dehydrogenase, Nature Communications 11 (1) (2020) 1–17, 2020 11.
[14] D.R. Wise, P.S. Ward, Shay JES, J.R. Cross, J.J. Gruber, U.M. Sachdeva, et al., Hypoxia promotes isocitrate dehydrogenase dependent carboxylation of α-ketoglutarate to citrate to support cell growth and viability, Proceedings of the National Academy of Sciences of the United States of America (2011) 19611–19616. Dec 6.
[15] AR Mullen WW Wheaton ES Jin Chen PHH LB Sullivan T Cheng et al Reductive carboxylation supports growth in tumour cells with defective mitochondria. n.d. Nature p. 385–8.
[16] J. Meiser, L. Krämer, S.C. Sapcariu, N. Battello, J. Ghelfi, A.F. D'Herouel, et al., Pro-inflammatory macrophages sustain pyruvate oxidation through pyruvate dehydrogenase for the synthesis of itaconate and to enable cytokine expression, J. Biol. Chem. 291 (8) (2016) 3932–3946.
[17] G.M. Tannahill, A.M. Curtis, J. Adamik, E.M. Palsson-McDermott, A.F. McGettrick, G. Goel, et al., Succinate is an inflammatory signal that induces IL-1β through HIF-1α, Nature 496 (7444) (2013 Apr) 238–242.
[18] J. Van den Bossche, J. Baardman, N.A. Otto, S. van der Velden, A.E. Neele, S. M. van den Berg, et al., Mitochondrial dysfunction prevents repolarization of inflammatory macrophages, Cell Rep. 17 (3) (2016 Oct 11) 684–696.
[19] A.M. Cameron, A. Castoldi, D.E. Sanin, L.J. Flachsmann, C.S. Field, D.J. Puleston, et al., Inflammatory macrophage dependence on NAD + salvage is a consequence of reactive oxygen species–mediated DNA damage, Nat. Immunol. 20 (2019) 420–432.
[20] J.S. Lewis, J.A. Lee, J.C.E. Underwood, A.L. Harris, C.E. Lewis, Macrophage responses to hypoxia: relevance to disease mechanisms, J. Leukoc. Biol. 66 (1999) 889–900.
[21] Y. Nonnenmacher, R. Palorini, A.F. d'Herouël, L. Krämer, M. Neumann-Schaal, F. Chiaradonna, et al., Analysis of mitochondrial metabolism in situ: combining stable isotope labeling with selective permeabilization, Metab. Eng. 1 (43) (2017 Sep) 147–155.
[22] S.M. Fendt, E.L. Bell, M.A. Keibler, B.A. Olenchock, J.R. Mayers, T.M. Wasylenko, et al., Reductive glutamine metabolism is a function of the α-ketoglutarate to citrate ratio in cells, NatureCommunications 4 (2013) 2236.
[23] V. Vijayan, P. Pradhan, L. Braud, H.R. Fuchs, F. Gueler, R. Motterlini, et al., Human and murine macrophages exhibit differential metabolic responses to lipopolysaccharide - a divergent role for glycolysis, Redox Biol. 1 (22) (2019 Apr), 101147.
[24] M.A. Selak, S.M. Armour, E.D. MacKenzie, H. Boulahbel, D.G. Watson, K. D. Mansfield, et al., Succinate links TCA cycle dysfunction to oncogenesis by inhibiting HIF-α prolyl hydroxylase, Cancer Cell. 7 (1) (2005 Jan 1) 77–85.
[25] N.C. Williams, D.G. Ryan, Costa ASH, E.L. Mills, M.P. Jedrychowski, S.M. Cloonan, et al., Signaling metabolite L-2-hydroxyglutarate activates the transcription factor HIF-1α in lipopolysaccharide-activated macrophages, The Journal of biological chemistry. J Biol Chem; 298 (2022).
[26] X. Du, H. Hu, The roles of 2-hydroxyglutarate, Front. Cell Dev. Biol. 26 (9) (2021 Mar) 486.
[27] R. Leonardi, C. Subramanian, S. Jackowski, C.O. Rock, Cancer-associated isocitrate dehydrogenase mutations inactivate NADPH-dependent reductive carboxylation, J. Biol. Chem. 287 (2012) 14615–14620.
[28] S.R. McKeown, Defining normoxia, physoxia and hypoxia in tumours—implications for treatment response, Br. J. Radiol. 87 (1035) (2014) 1–12. Mar 1;87(1035).
[29] A.R. Mullen, Z. Hu, X. Shi, L. Jiang, L.K. Boroughs, Z. Kovacs, et al., Oxidation of alpha-ketoglutarate is required for reductive carboxylation in cancer cells with mitochondrial defects, Cell Rep. 7 (5) (2014 Jun 12) 1679–1690.
[30] J. Domínguez-Andrés, B. Novakovic, Y. Li, B.P. Scicluna, M.S. Gresnigt, R.J. W. Arts, et al., The itaconate pathway is a central regulatory node linking innate immune tolerance and trained immunity, Cell Metab. 29 (1) (2019) 211–220.e5.
[31] Y. Li, P. Zhang, C. Wang, C. Han, J. Meng, X. Liu, et al., Immune responsive gene 1 (IRG1) promotes endotoxin tolerance by increasing A20 expression in macrophages through reactive oxygen species, J. Biol. Chem. 288 (23) (2013) 16225–16234.
[32] E.L. Mills, B. Kelly, A. Logan, Costa ASH, M. Varma, C.E. Bryant, et al., Succinate dehydrogenase supports metabolic repurposing of mitochondria to drive inflammatory macrophages, Cell 167 (2016), p. 457-470.e13.
[33] K.E. de Goede, K.J. Harber, F.S. Gorki, S.G.S. Verberk, L.A. Groh, E.D. Keuning, et al., D-2-hydroxyglutarate is an anti-inflammatory immunometabolite that accumulates in macrophages after TLR4 activation, Biochim. Biophys. Acta, Mol. Basis Dis. 1868 (9) (2022 Sep 1), 166427.
[34] L. Zhou, F. Wang, R. Sun, X. Chen, M. Zhang, Q. Xu, et al., SIRT5 promotes IDH2 desuccinylation and G6PD deglutarylation to enhance cellular antioxidant defense, EMBO Rep. 17 (2016) 811.
[35] A.R. Stram, R.M. Payne, Post-translational modifications in mitochondria: protein signaling in the powerhouse, Cell. Mol. Life Sci. 73 (2016) 4063–4073.
[36] L.S. Pike, A.L. Smift, N.J. Croteau, D.A. Ferrick, M. Wu, Inhibition of fatty acid oxidation by etomoxir impairs NADPH production and increases reactive oxygen species resulting in ATP depletion and cell death in human glioblastoma cells, Biochim. Biophys. Acta 1807 (6) (2011) 726–734.
[37] K. Hiller, J. Hangebrauk, C. Jäger, J. Spura, K. Schreiber, D. Schomburg, MetaboliteDetector: comprehensive analysis tool for targeted and nontargeted GC/MS based metabolome analysis, Anal. Chem. 81 (9) (2009 May 1) 3429–3439.
[38] D. Brenner, M. Brechmann, S. Röhling, M. Tapernoux, T. Mock, D. Winter, et al., Phosphorylation of CARMA1 by HPK1 is critical for NF-κB activation in T cells, Proc. Natl. Acad. Sci. U. S. A. 106 (34) (2009 Aug 25) 14508–14513.